Torque and Reactive Power Control of a Doubly-Fed Induction Machine by Position Sensorless Scheme

Wei Cheng
Student Member, IEEE

Longya Xu
Senior Member, IEEE

The Ohio State University
Department of Electrical Engineering
2015 Neil Avenue
Columbus, Ohio 43210

I. Introduction

Doubly fed wound rotor induction machine with vector control is very attractive to the high performance, variable speed drive and generating applications[1-3]. In variable speed drive application, the so-called slip power recovering scheme is a common practice where the power due to the rotor slip below/above synchronous speed is recovered to/supplied from the power source, resulting a high efficiency variable speed system. In variable speed generating application, the doubly fed induction machine is most suited for variable-speed constant-frequency generating systems in which the speed of the prime mover is allowed to vary within a certain range (sub- and super synchronous speed), but the output electrical power is always maintained at a constant frequency. In such a case, the doubly fed induction machine is actually in the dual mode of variable speed drive system.

The fundamental feature of the doubly fed induction machine system, including the drive and generating systems, is that the power processed by the power converter is only a small fraction of the total system power. Therefore, for a very large rating system it is possible to use a high-frequency switching PWM converter to achieve high performance, such as fast dynamic response, low harmonic distortion, high efficiency, etc., without cost penalty. However, a high resolution rotor position sensor is generally needed for the proper operation of the doubly fed induction machine systems.

Research has been very active in recent years to eliminate position sensors in field orientation controlled cage rotor induction machine and the results are promising[4-6]. In a cage rotor induction machine, the rotor current is passively induced and the rotor field is subsequently defined by the induced current. Yet, for the doubly excited induction machine the rotor field is explicitly defined by the external excitation source which requires synchronization with respect to the stator field. Therefore, without using a shaft position sensor, vector or field orientation control of a doubly fed induction machine is more complicated than that of a singly-excited cage rotor machine.

In this paper, a novel control strategy to realize torque and reactive power control of a doubly excited induction machine using position sensorless scheme is proposed. Compared to the other position sensorless schemes for doubly fed machine, the proposed control method uses only the rotor voltages and currents as the feed back signals, which substantially reduces the costs and enhances relibility of the position sensorless control scheme of the doubly fed AC machine[8,9]. Independent control of torque and reactive power is also possible, and the doubly fed system can achieve unity or leading power factor, in addition to variable speed operation.

II. Configuration and Operation Principles

A. Configuration of Doubly Fed Induction Machine System

The configuration of a variable speed doubly fed induction machine system is shown in Fig. 1.

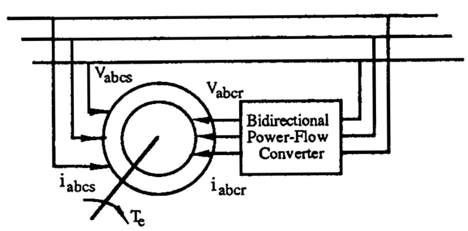

Fig. 1 Configuration of Doubly fed Induction Machine system

The major component of the system is a wound rotor induction machine which needs to be excited at both the stator and rotor terminals. It is common practice that the stator winding is connected to the AC power supply directly, while the rotor winding is connected to the power supply through a variable frequency power converter. To obtain sub- and sup-synchronous speed operation, the power converter of the rotor winding must be able to handle slip power in both directions [2] using a PWM voltage source inverter. Among the three power flow ports, i.e. the stator terminals, the rotor terminals, and the rotor shaft, the rotor terminals act as the energy regulating port, balancing the power flow of the entire system. For example, when the shaft speed is below synchronous speed, a small portion of power is subtracted from the system through the rotor terminals so that the power input to the system through the stator winding is balanced by the power output from both

0-7803-1993-1/94 $4.00 © 1994 IEEE

mechanical shaft and the rotor circuit. Similarly, when the shaft speed is above synchronous speed, a small portion of power is added to the system through the rotor circuit. While the example is given in terms of motor operation, it is straightforward to prove that for generator operation, the rotor circuit functions in a similar manner.

B. Basic Equations and Operation Principles

The operation principle of the variable speed doubly fed induction machine can be conveniently analyzed by the classical rotating field theory with the well-known d-q-0 transformation. By inspection, the stator and rotor equations are written as follows in the matrix form.

$$\underline{v}_{abcs} = r_s \underline{i}_{abcs} + \frac{d\underline{\lambda}_{abcs}}{dt} \quad (1)$$

$$\underline{v}_{abcr} = r_r \underline{i}_{abcr} + \frac{d\underline{\lambda}_{abcr}}{dt} \quad (2)$$

After the d-q-0 transformation, the equations, in the synchronous reference frame, are

$$\underline{v}_{dqs} = r_s \underline{i}_{dqs} + \frac{d\underline{\lambda}_{dqs}}{dt} + \underline{\omega}_e \times \underline{\lambda}_{dqs} \quad (3)$$

$$\underline{v}_{dqr} = r_r \underline{i}_{dqr} + \frac{d\underline{\lambda}_{dqr}}{dt} + (\underline{\omega}_e - \underline{\omega}_r) \times \underline{\lambda}_{dqr} \quad (4)$$

where ω_e is the speed of the synchronous reference frame, and ω_r is the rotor speed.

The torque equation becomes

$$T_e = \frac{3}{2}\frac{p}{2} |\lambda_{qdm}| \, |i_{qdr}| \sin \delta \quad (5)$$

wherein $\underline{\lambda}_{qdm} = \underline{\lambda}_{qds} - \underline{i}_{qds} L_{\ell s}$

and $\underline{\lambda}_{qdm} = \underline{\lambda}_{qdr} - \underline{i}_{qdr} L_{\ell r}$ (6)

In Eq. (5), δ is the spatial angle between the airgap flux and rotor current vectors (named torque angle in this paper) seen in the synchronous reference frame. With the alignment of the airgap flux to the d-axis of the reference frame, we will have

$$\lambda_{qdm} = \lambda_{dm} \quad \text{and} \quad \lambda_{qm} = 0. \quad (7)$$

The torque equation is reduced to

$$T_e = \frac{3}{2}\frac{p}{2} |\lambda_{dm}| \, |i_{qr}| \quad (8)$$

In order for rotor current vector in synchronization with the stator current vector, the frequency of the rotor current, ω_s, must satisfy the slip frequency constraint

$$\omega_s = \omega_e - \omega_r \quad (9)$$

Furthermore, for field orientation control, δ must be maintained at 90°, or equivalently, the current vector has to maintain orthogonal to the airgap flux. For a general vector control, the rotor current vector is controlled with a predetermined angle with respect to the airgap flux. It is because of Eq. (9) and the field orientation or vector control that the rotor speed and position must be measured (or estimated) instantaneously so that the rotor current vector can be correctly positioned.

C. Reactive Power Control Through Rotor Currents

The reactive power of the doubly fed induction machine system can be controlled through the rotor current vector to realize unity or leading power factor operation. Assuming that the required reactive power to the stator is Q_s which can be expressed in the d-q-0 reference frame as

$$Q_s = \frac{3}{2}\frac{p}{2} (v_{qs} i_{ds} - v_{ds} i_{qs}) \quad (10)$$

The reactive power Q_s can be referred to the rotor side and expressed in terms of rotor quantities as

$$Q_s = \frac{3}{2} \omega_e \left(\frac{L_s \lambda_m^2}{L_m^2} - \lambda_m i_{dr} + L_{\ell s} (i_{dr}^2 + i_{qr}^2 - 2 \lambda_m i_{dr}) \right) \quad (11)$$

or

$$Q_s = \frac{3}{2} \omega_e \left(\frac{L_s \lambda_m^2}{L_m^2} - \lambda_m i_{dr} \right) \quad (12)$$

if the reactive power consumed by the stator leakage inductance is very small and neglected.

In a doubly fed induction machine the airgap flux is determined largely by the stator voltage which has a constant magnitude and frequency. Hence, it is reasonable to further assume that the airgap flux is constant. According to Eqs. (11) and (12), if the rotor current i_{dr} is controlled, the reactive power or the power factor can be controlled. Again, for reactive power control, the rotor speed and the rotor position must be known for the rotor current vector projection. (see Appendix)

III. Estimation of Torque Angle and Rotor Speed

As discussed above, in order to have precise control over the torque and reactive power (or power factor) of the doubly fed induction machine, we need to maintain a controllable torque angle, δ, or a controllable rotor current vector, $|i_{qdr}|$. For the doubly fed induction machine system using a high resolution shaft encoder, the rotor position is constantly sensed to ensure that the required slip frequency, ω_s, satisfies the equation $\omega_s = \omega_e - \omega_r$. The orientation of the rotor current vector is realized by the final tuning of the slip frequency so that the command currents i_{qr} and i_{dr} are projected orthogonal and parallel to the airgap flux respectively. In the following sections, we will discuss how i_{qr} and i_{dr} are projected to the right position without the use of a costly position sensor.

A. Estimation of Torque Angle

It is extremely important to realize that the electromagnetic torque can be viewed as the result of the interaction between rotor current and airgap flux, *regardless of the selection of the reference frame*. That is, Equations

$$T_e = \frac{3}{2}\frac{p}{2}(\lambda_{dm} i_{qr} - \lambda_{qm} i_{dr})$$
$$= \frac{3}{2}\frac{p}{2}|\lambda_{qdm}|\,|i_{qdr}|\sin\delta \quad (13)$$

and
$$T_e = \frac{3}{2}\frac{p}{2}(\lambda_{ym} i_{xr} - \lambda_{xm} i_{yr})$$
$$= \frac{3}{2}\frac{p}{2}|\lambda_{xym}|\,|i_{xyr}|\sin\delta \quad (14)$$

are equivalent. In Eqs. (13-14), we have used subscripts of d-q, and x-y to differentiate the selection of the reference frames tied to the synchronous and rotor circuit frame respectively. Since Eqs. (13-14) are equivalent, observation of the magnitudes of flux and current, as well as the electromagnetic torque, are independent of the reference frame selection. One can estimate the torque angle in one reference frame, and then use the estimated results in other reference frames. Furthermore, the airgap flux can be estimated from either the stator, rotor or combined circuit. Therefore, one can always choose the most convenient circuit, that of the stator or rotor, in the most convenient reference frame, the rotor or synchronous frame, to compute the magnitudes of the flux and current, and the torque angle δ.

In the position sensorless control strategy proposed in this paper, the rotor currents and voltages are used as the basic input variables to compute the torque angle, because the rotor variables are already available for the purpose of current regulation. Assuming that the reference frame is tied to the rotor axis, the torque angle and the flux magnitude together with the current magnitude can be estimated by the measured rotor voltages and currents according to the following equations:

$$\hat{\lambda}_{xm} = \int (v_{xr} - r_r i_{xr})\,dt - L_{\ell r} i_{xr} \quad (15)$$

$$\hat{\lambda}_{ym} = \int (v_{yr} - r_r i_{yr})\,dt - L_{\ell r} i_{yr} \quad (16)$$

$$\hat{\lambda}_m = \sqrt{\hat{\lambda}_{xm}^2 + \hat{\lambda}_{ym}^2} \quad (17)$$

$$i_r = \sqrt{i_{xm}^2 + i_{ym}^2} \quad (18)$$

Thus, according to Eq. 14, the sine of the torque angle is:

$$\sin\hat{\delta} = \frac{\hat{\lambda}_{ym} i_{xr} - \hat{\lambda}_{xm} i_{yr}}{\hat{\lambda}_m i_r} \quad (19)$$

In Eqs. (15) through (19), $\hat{\delta}$, $\hat{\lambda}_{xm}$, $\hat{\lambda}_{ym}$, and $\hat{\lambda}_m$ are used to indicate that they are the estimated values from the estimator. Note, however, that $\sin\hat{\delta}$ alone is not sufficient to uniquely determine the value of $\hat{\delta}$, since the inverse of a sine function is dual-valued. Interpreting this observation to the machine physics, we can say that the information contained in the electromagnetic torque or active power can not uniquely determine the torque angle. It is evident that additional information is necessary. In effect, by computing a quantity related to the instantaneous reactive power, $\cos\delta$ can be found by the following equation:

$$\cos\hat{\delta} = \frac{\hat{\lambda}_{ym} i_{yr} + \hat{\lambda}_{xm} i_{xr}}{\hat{\lambda}_m i_r} \quad (20)$$

Taking the inverse of $\sin\delta$ and $\cos\delta$ terms, the torque angle δ is uniquely determined. Similar to the computation of sine term, the needed inputs for Eq. (20) are rotor side variables which are readily available and no additional sensing is needed.

B. Control of Torque Angle

It is interesting to note that by using the rotor voltages and currents, the torque angle δ is estimated without any transformation. Nevertheless, the estimated angle $\hat{\delta}$ can be used in any other reference frames. Using the estimated angle of $\hat{\delta}$ as the feedback variable, it is possible to force the actual δ to follow the desired value. The scheme of the torque angle estimation and control is summarized as shown in Fig. 2. In the control block of Fig. 2, a voltage controlled oscillator (VCO) with high gain is used to generate a desired slip frequency so as to converge the actual torque angle to the desired

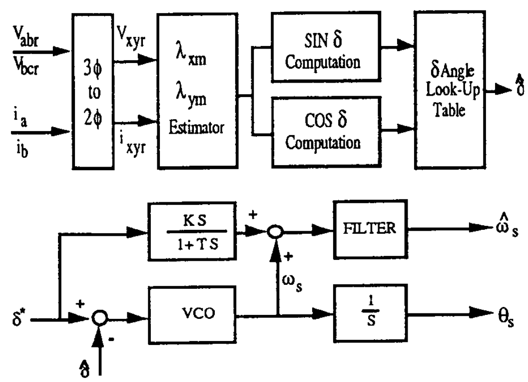

Fig. 2 Estimation and Control of Torque Angle

one. It is in this way that the torque and reactive power control of the doubly fed induction machine is properly achieved. The torque angle control scheme can be best illustrated by the phasor diagram shown in Fig. 3. Note that as soon as an error in the torque angle is detected by the estimator, for example $\hat{\delta} < \delta^*$ as shown in the phasor diagram, the VCO based controller will immediately slow down the slip frequency so that θ_s is reduced. As a result, the torque angle increases. To make the current regulators in the synchronous reference frame function properly, i. e. to force i_{qr} to increase and i_{dr} to decrease, it is a wise choice to transform the measured rotor current to the synchronous reference frame by

$$i_{dr} = i_{xr}\cos\theta_s + i_{yr}\sin\theta_s$$

$$i_{qr} = -i_{xr}\sin\theta_s + i_{yr}\cos\theta_s$$

and then use them as the feedback signals.

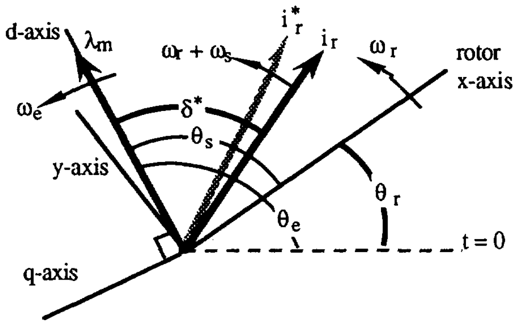

Fig. 3 Phasor Diagram of Torque Angle Control

C. Estimation and Control of Rotor Speed

Integrating the torque angle estimation and control schemes into the system, the rotor speed can be estimated conveniently. Recall that we have forced the torque angle to the command value continuously. This simply implies that the rotor current vector is synchronized with respect to the stator field, satisfying the slip frequency constraint $\omega_s = \omega_e - \omega_r$. Consequently, the rotor speed can be estimated by using the slip frequency constraint equation $\omega_r = \omega_e - \omega_s$, where ω_e and ω_s are known quantities.

Adding the rotor speed estimation and control to the torque angle control loop, the block diagram of the overall system is obtained as shown in Fig. 4

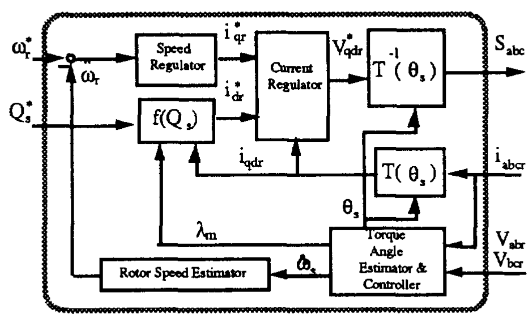

Fig. 4 Block Diagram of the Proposed Controller

The portion enclosed in the box can be implemented by software and executed in a digital signal processor conveniently.

Note that the rotor current vector is not always synchronized with respect to the stator field or airgap field. The momentary lose of synchronization between the rotor current and airgap field is particularly true, and is actually necessary for the changes of the torque and/or reactive power command. In such a case, an error will occur in rotor speed estimation. To correct this error, a feed forward signal as shown in Fig. 2 may be helpful to compensate the temporarily lose of the synchronization.

IV. Results of Computer Simulation

The principles and control scheme of the position sensorless controlled doubly fed induction machine described in Fig. 4 is implemented by a computer program and then the performance is investigated. The specifications of the doubly fed induction machine used in the computer simulation are shown in Table 1.

For the doubly fed induction machine under investigation, the stator is fed from a three phase AC supply at 60 Hz from the utility lines. The rotor current is provided by a CRPWM power converter. First, the estimation scheme of the torque angle is checked and the results are shown in Figs. 5(a) through 5(f). Fig 5(a) shows the torque angle command, δ^*; (b) the actual rotor speed; (c) the estimated $\sin\delta$; (d) the estimated $\cos\delta$; (e) the estimated torque angle; and (f) the estimated rotor speed. Comparing Figs. 5(a) with 5(e), it is evident that the torque angle is accurately estimated. The rotor is accelerated steadily, covering both the sub- and sup-synchronous speed zones. Similar results are shown in the same figures when the machine is decelerated. As shown in Figs. 5(b) and 5(f), the estimated motor speed is very close to the actual one.

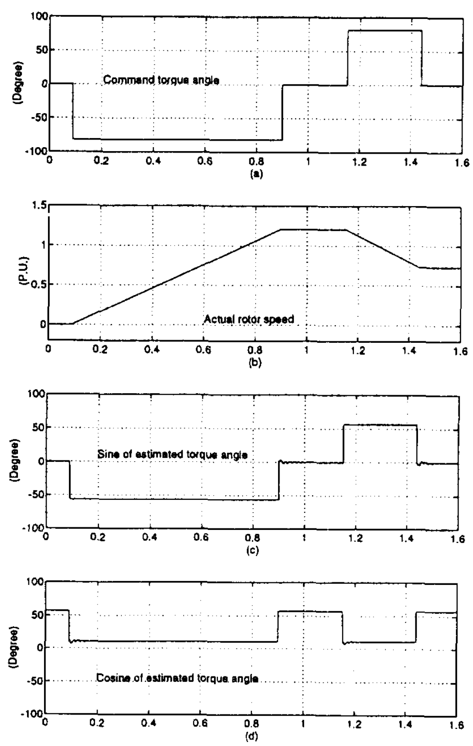

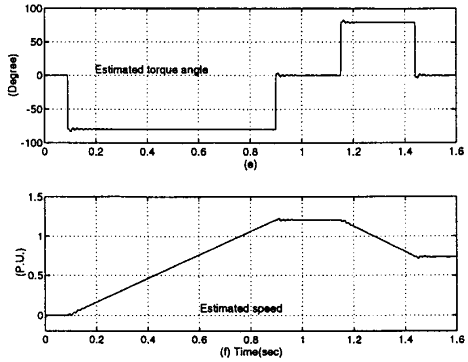

Fig. 5 Simulation Results of Torque Angle and Speed Estimation

Fig. 6 shows the result of the closed loop speed control. As discussed previously, in the power angle controller, a slip frequency command is generated to synchronize the rotor current vector with respect to the stator field. This implies that the correctly generated slip frequency can be used readily for rotor speed estimation. That is, $\omega_r = \omega_e - \omega_s$ where ω_e and ω_s are known variables. With the virtually overlapped two traces, Fig. 6(a) shows the command and the actual rotor speed; Fig. 6(b) shows the estimated rotor speed which is used as the feedback variable; and Fig. 6(c) shows the rotor phase current.

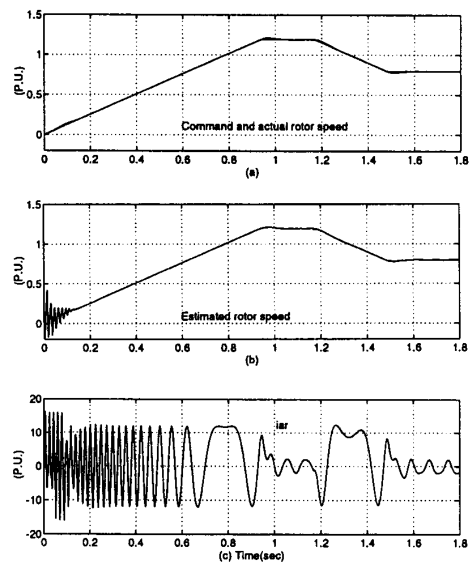

Fig. 6 Simulation Results of Speed Control

The third simulation investigates the reactive power control of the doubly fed induction machine by the position sensorless control scheme, and the results are shown in Fig. 7. Two levels of i_{dr} are applied to change the power factor, which are clearly achieved by the position sensorless control method. In addition, i_{qr} is not affected indicating a decoupled reactive power control from the torque control.

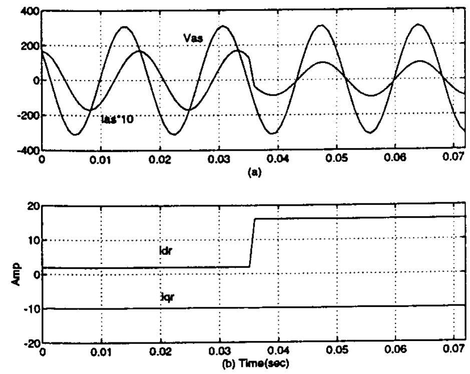

Fig. 7 Decoupled Control of Reactive Power

V. Experimental Results

To substantiate the theoretical analysis and computer simulation, the control algorithm has been realized by a general purpose Motorola DSP56000 system and tested on a doubly fed variable speed drive, with the machine specifications the same as those of the simulated one, implemented at The Ohio State University. Only four A/D channels are used on the rotor circuit for torque angle estimation and control.

Torque angle estimation is tested first and the results are shown in Fig. 8. In the test, the machine is under vector control using a rotor position encoder. It can be observed that when the accelerating torque is applied the estimated torque angle is about -90° and when the decelerating torque is applied the torque angle is about 90°, both are very well matched to the actual toque angles. The phase current is shown as the third trace, clearly indicating the correspondence of the magnitude versus that of the phase current. It should be pointed out, however, that when the torque is very small, during the interval of constant speed and low phase current, the torque angle observation curve has many ripples. This is because the input signals to the torque angle estimator are too weak and the estimation is sensitive to the input errors.

Fig. 9 shows the experimental results using the estimated torque angle and speed as the feedback signals for torque and speed regulation. In this case, the doubly fed machine is truly under the position sensorless control. As indicated by the testing results, the torque angle and speed estimation are applied to the torque control and speed regulation successfully. It is interesting to compare the phase current of this figure to that of the previous one. Note that the phase current magnitude at light load with position sensorless control is much larger than that with position sensor. This is because, as describe above, the torque angle observation at light load is easily subject to the errors for the low signal/noise ratio.

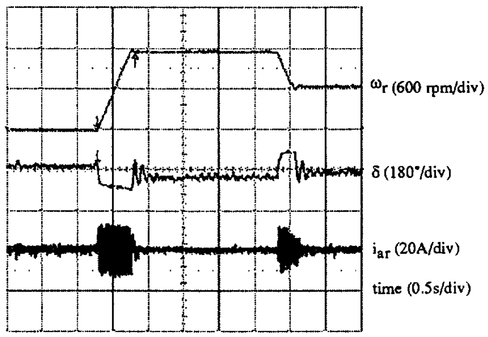

Fig. 8 Testing Results of Torque Angle Estimation

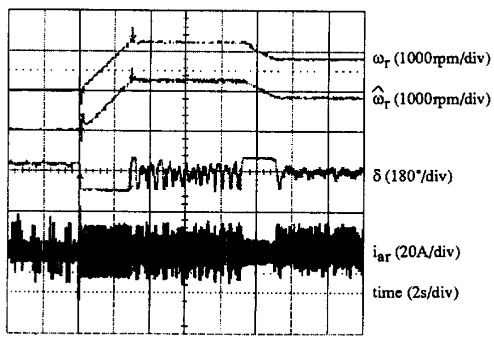

Fig. 9 Testing Results of Speed Control without Position sensor

Fig. 10 is the experimental results of decoupled reactive power control using position sensorless scheme. The power factor of the stator circuit is evidently boosted to almost unity when a step magnetizing current i_{dr} is applied while the torque is not affected.

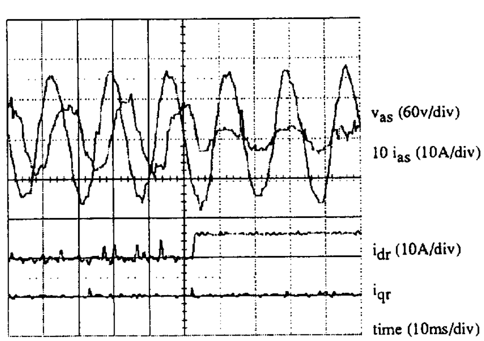

Fig. 10 Reactive Power Control

In experimental testing, the torque angle estimation algorithm is tested over a wide speed range covering both sub- and super synchronous speed and the results are shown in Fig. 11. It can be seen that when the rotor crossing synchronous speed, a big dip appears on the torque angle estimation curve, showing a difficulty of estimating torque angle at very low frequency. This is actually a dual problem met in the singly fed induction machine when the rotor speed is very low, or equivalently, the excitation frequency approaches zero. While the torque angle estimation at low frequency itself constitutes a major research topic and is out of the scope of this paper, more advanced control algorithm does show the light that the problem could be overcome as described in [10].

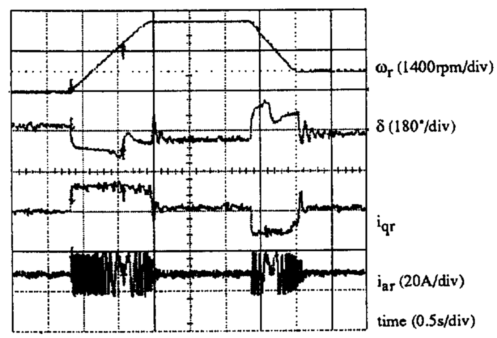

Fig. 11 Testing Results of Torque Angle Estimation When Rotor Crossing Synchronous Speed

VI. Conclusions

A position sensorless scheme is proposed for the doubly fed induction machine system using only the rotor side variables as the measured signals. The principles associated with this particular position sensorless control are presented and discussed. The theoretical results are verified by computer simulation and lab experiments. The following conclusions are reached:

1). The torque angle δ can be estimated satisfactorily by the method suggested except when the rotor frequency is very low. The angle observed contains information of the rotor mechanical speed and angle, together with those of the rotor excitation;

2). For torque angle estimation in position sensorless scheme, information related to both torque (active power) and reactive power must be used to uniquely determine the torque angle. The estimation is independent to the selection of reference frames, and to the rotor or stator circuits.

3). Torque angle control technique can be used to replace rotor position sensor for high performance vector control of doubly-excited AC machines. Independent control of the reactive power can also be achieved by the position sensorless control scheme.

4). To use the position sensorless method for rotor speed estimation and control, the estimation is subject to an error introduced by the very low operating frequency or whenever the load torque is very light.

It should be pointed out that although the position sensorless method presented in this paper is applied to the doubly fed induction machine, the mechanism described is applicable to the other doubly excited machines including conventional synchronous machine, PM machine, synchronous reluctance machine, and the newly developed doubly excited brushless reluctance machine. In the future work, more advanced algorithm will be included in the torque angle estimation to account for parameter variation at low frequency. Further, intelligent control approach, such as fuzzy logic control, can be added to the slip frequency generator to enhance robustness and simplify the controller.

References

1). S. R. Doradla, S. Shakravorty, and K. E. Hole, "A New Slip Recovery Scheme with Improved Supply Power Factor," IEEE Trans. on Power Electronics, vol. 2, No. 2, April, 1988

2). L. Xu and Yifan Tang, "A Novel Variable Speed Constant Frequency Wind-Power Generating System Using Doubly-Excited Brushless Reluctance Machine", IEEE/IAS Annual Meeting, Oct. Houston, 1992.

3). L. Refoufi, P. Pillay and M. R. Harris, "A Chopper-Controlled Slip Energy Recovery Induction Motor Drive," IEEE/PES Summer Meeting, Seattle, 1992

4) Hirokazu Tajima and Yoichi Hori, "Speed Sensorless Field Orientation Control of the Induction Machine," IEEE/IAS Transactions, Vol. 29, No. 1, Jan/Feb, pp 175-180

5) T. Ohtani, N. Takata and K. Tanata, "Indirect Vector Control Without Shaft Encoder," IEEE/IAS Annual Meeting Record, 1989, pp 500-507

6) F. Zheng amd T. Fukao, "Robust Speed Identification for Speed Sensorless Vector Control of Induction Motors," IEEE/IAS Annual Meeting, 1993, pp 419-426

7). L. Xu and Y. Tang, "Stator Field Oriented Control of Doubly-Excited Induction Machine in Wind Power Generating System", 35th Mid West Symposium on Circuit and System, Washington D. C., Aug. 1992.

8). Y. Liao and C. Sun, "A Low Cost, Robust Position Sensorless Control Scheme for Doubly-Fed Reluctance Motor Drives," IEEE/IAS Annual Meeting 1993, pp 437-444

9) A. B. Plunkett and F. G. Turnbull "Load-Commutated Inverter/Synchronous Motor Drive without a Shaft Position Sensor", IEEE/IAS Transaction, Vol. IA-15 No. 1, Jan/Feb. 1979, pp 63-71

10) Y. Tang and L. Xu, "Fuzzy Logic Application for Intelligent Control of a Variable Speed Drive", IEEE/PES Winter Meeting, Feb., 1994, New York, to appear on IEEE Transactions on Energy Conversion.

Table 1: Specifications of the Induction Machine

Voltage 220 volts	Current 14.8 amps
Rated speed 1725 rpm	R_s = 1.11 ohms
R_r = 0.3 Ohms	x_m = 18 ohms
$x_{\ell s} = x_{\ell r}$ = 0.77 ohms	

Appendix:

Reactive Power Flow of the Doubly Fed Induction Machine

Reactive power flow in the doubly fed induction machine is derived in this appendix. Note that the basic equations of a doubly fed induction machine are expressed in the synchronous reference frame as

$$v_{ds} = r_s\, i_{ds} - \omega_e \lambda_{qs} + \frac{d\lambda_{ds}}{dt} \quad \text{(A-1)}$$

$$v_{qs} = r_s\, i_{qs} + \omega_e \lambda_{ds} + \frac{d\lambda_{qs}}{dt} \quad \text{(A-2)}$$

$$\lambda_{ds} = L_{\ell s}\, i_{ds} + \lambda_{dm} \quad \text{(A-3)}$$

$$\lambda_{qs} = L_{\ell s}\, i_{qs} + \lambda_{qm} \quad \text{(A-4)}$$

If the d-axis of the reference frame is aligned with the airgap flux, the next two equations follow.

$$\lambda_{qm} = 0 = L_m (i_{qs} + i_{qr}) \quad \text{(A-5)}$$

$$\lambda_{dm} = \lambda_m = L_m (i_{ds} + i_{dr}) \quad \text{(A-6)}$$

The reactive power flow into the stator winding is

$$Q_s = \frac{3}{2} (v_{qs}\, i_{ds} - v_{ds}\, i_{qs}) \quad \text{(A-7)}$$

Substituting Equations (A-5) and (A-6) into Eqs. (A-1) through (A-4), and making use of the results in Eq. (A-7), we have

$$Q_s = \frac{3}{2} \omega_e \lambda_m i_{ds} + \frac{3}{2} \omega_e L_{\ell s} (i_{ds}^2 + i_{qs}^2) \quad \text{(A-8)}$$

Eq. (A-8) can be expressed purely in terms of rotor side variables

$$Q_s = \frac{3}{2} \omega_e \left(\frac{L_s \lambda_m^2}{L_m^2} - \lambda_m i_{dr} + L_{\ell s} (i_{dr}^2 + i_{qr}^2 - 2 \lambda_m i_{dr}) \right) \quad \text{(A-9)}$$

Furthermore, the reactive power consumed by the leakage inductance is very small, and can be neglected. Therefore,

$$Q_s = \frac{3}{2} \omega_e \left(\frac{L_s \lambda_m^2}{L_m^2} - \lambda_m i_{dr} \right) \quad \text{(A-10)}$$

If the magnitude of the airgap flux λ_m is stable, which is true for the doubly fed induction machine in steady state, then the desired amount of reactive power flow into the stator can be controlled by controlling i_{dr} as indicated by the Equation.